Catalysis Today 413-415 (2023) 113942

Contents lists available at ScienceDirect

Catalysis Today

journal homepage: www.elsevier.com/locate/cattod

Photocatalytic degradation of methylisothiazolinone in water by TiO_2 and TiO_2/persulfate systems with simulated solar radiation

Pilar Gómez-Rodríguez [a], Paola Calza [b], Debora Fabbri [b], Claudio Medana [b], Rafael van-Grieken [a], María-José López-Muñoz [a,*]

[a] Departamento de Tecnología Química y Ambiental, Universidad Rey Juan Carlos, C/Tulipán s/n, 28933 Móstoles, Spain
[b] Department of Chemistry, University of Turin, Via P. Giuria 7, 10125 Torino, Italy

ARTICLE INFO

Keywords:
Methylisothiazolinone
TiO_2
Photocatalytic treatment
Water matrix
Persulfate activation

ABSTRACT

The photocatalytic decomposition of methylisothiazolinone (MIT) in water was successfully attained with TiO_2 and TiO_2/persulfate systems under simulated solar irradiation. The TiO_2 catalysts were synthesized by sol-gel process, controlling the hydrolysis rate of titanium n-butoxide by two procedures: external addition of water and *in situ* production of water *via* esterification between ethanol and a carboxylic acid. Crystalline structure, morphology and textural properties of materials were characterized by XRD, SEM and N_2 adsorption-desorption isotherms. The photocatalytic activity of the obtained catalysts for MIT degradation was proved to be significantly dependent on both the procedure of water provision for the alkoxide hydrolysis and the calcination temperature. Adding persulfate (PS) to the system resulted in a great enhancement of the MIT degradation rate, which was kept in different water matrices due to a synergistic effect between the titania catalysts and PS activation. MIT transformation products (TPs) were identified by HPLC-HRMS and a mechanism for MIT degradation was proposed. Total Organic Carbon and toxicity measurements established the complete MIT mineralization and non-toxicity of the water solution after the photocatalytic treatment.

1. Introduction

Isothiazolinones are a group of biocides commonly employed as preservatives in aqua-based industrial products as well as in cosmetics and skin care products due to their ability to control microbial growth [1]. Despite the effectiveness of their antibacterial and antifungal applications, negative consequences in environment and human health have caught the attention of research in recent years. Even in very low concentrations, isothiazolinones have been reported to be high sensitizers and skin irritants, causing several cases of allergic contact dermatitis when they are present in personal care products [2]. Furthermore, the presence of these compounds in industrial and domestic wastewater has a potential ecotoxicity risk, affecting living species, such as fishes and other aquatic organisms [3]. The increasing use of these compounds has become a new source of water contamination which derives from both the application itself and the contaminated wastes of manufacturing industries.

Preservative methylisothiazolinone (MIT) is one of the most employed isothiazolinone derivatives in the cosmetic industry, frequently disposed as a 3:1 mixture with chloro-methylisothiazolinone (CMIT) under the commercial name of Kathon CG. European legislation has established the maximum concentration of this mixture in cosmetics to 0.0015% (w/w) [4].

To date, there are few studies regarding the removal of MIT from water and the identification of its transformation products. For that purpose, in the present work heterogeneous photocatalysis has been investigated as it is considered an efficient, economic, and eco-friendly technology for removing harmful compounds from water [5]. In those processes TiO_2 has been widely employed due to its great potential as a photocatalyst, low-cost, thermodynamic and chemical stability in water solution, and non-toxicity of products upon decomposition [6,7].

The fundamentals of heterogeneous photocatalysis with TiO_2 are well known. The exposure of titania particles to light irradiation leads to the absorption of photons whose energy level overcomes the bandgap energy of the semiconductor, producing the excitation of electrons in the valence band (VB) and their subsequent migration to the conduction band (CB) (e^-_{CB}) leaving positive holes (h^+_{VB}) in the VB. Consequently, most of charge carriers recombine with the release of energy but some of

* Corresponding author.
E-mail address: mariajose.lopez@urjc.es (M.-J. López-Muñoz).

https://doi.org/10.1016/j.cattod.2022.11.003
Received 31 August 2022; Received in revised form 12 October 2022; Accepted 1 November 2022
Available online 11 November 2022

them can reach the semiconductor surface where they can either recombine or react with different species. The photoexcited electrons can accomplish the reduction of adsorbed O_2 whereas positive holes can oxidize water molecules producing $HO^{\bullet}$ radicals, species able to oxidize organic contaminants to H_2O and CO_2 ($HO^{\bullet}$, E^0 =2.8 V *vs* NHE, in standard conditions). Thus, the success of the process is tightly related to the efficient suppression of the e^-/h^+ recombination at the catalyst surface [8,9].

In that way, the addition of electron acceptors stronger than oxygen could benefit the photocatalysis performance, decreasing the e^-/h^+ recombination rate. Introducing persulfate (PS, $S_2O_8^{2-}$) into the TiO_2 system can be an alternative for enhancing the photocatalyst activity as PS can inhibit photo-generated charge carriers recombination through the capture of the photo-induced electrons of the TiO_2 conduction band (e_{CB}^-) with generation of $SO_4^{\bullet-}$ radicals (Eq. (1)), which have a high redox potential (E^0 =2.6 V *vs* NHE, in standard conditions) [9,10]. Furthermore, those radicals have a longer half-life in comparison to $HO^{\bullet}$ ($t_{1/2}$ =30–40 μs *vs* $t_{1/2}$ =20 ns, respectively) [11], which favors the contact and mass transfer between $SO_4^{\bullet-}$ radicals and the pollutant. Thus, the formation of both hydroxyl and sulfate radicals would lead to a great oxidizing capacity of the system, promoting a highly efficient degradation of organic contaminants in water under light irradiation.

$$S_2O_8^{2-} + e_{CB}^- \rightarrow SO_4^{2-} + SO_4^{\bullet-} \quad (1)$$

The generation of $SO_4^{\bullet-}$ from PS can be accomplished through different activation methods that require the use of heat, ultrasound, UV-radiation, and transition metal ions. In those terms, the efficient combination of UV/TiO_2/PS has been investigated for enhancing the photocatalytic activity of TiO_2 [12], but there are no previous studies reporting isothiazolinones degradation through PS activation by TiO_2.

In this work, we report the photocatalytic activity of different homemade TiO_2 samples and their ability for PS activation for MIT degradation, using different water matrices. TiO_2 samples were prepared by a traditional and modified sol-gel methods and the influence of the synthesis parameters on their photocatalytic activity was assessed for the isothiazolinone removal. TPs formed throughout the reaction were identified *via* HPLC combined with an ESI LTQ Orbitrap and the MIT reaction pathway in water was proposed.

2. Materials and methods

2.1. Preparation of TiO_2 catalysts

2.1.1. External addition of water

This procedure was based on a previous work [13]. Two solutions, A and B, were prepared. In solution A 0.058 mol of titanium (IV) butoxide (Sigma-Aldrich, 97%) were added to 0.685 mol of absolute ethanol (VWR chemicals, 99.98%) and stirred until obtaining a homogeneous yellow solution. In solution B, 1.108 mol of ultrapure water were mixed with 0.343 mol of absolute ethanol and kept at 273 K or 343 K. Then, solution A was added dropwise to solution B, promoting a rapid formation of a white gel which was filtered, cleaned with absolute ethanol, and dried overnight at 353 K in air atmosphere, obtaining a white powder which was calcined at 823 and 923 K for 6 h, with a temperature rate of 1.8 K min^{-1}.

2.1.2. In-situ production of water via esterification reaction

The method followed was based on a procedure described elsewhere [14]. Briefly, 0.109 mol of titanium (IV) butoxide were added to 1.284 mol of absolute ethanol. The mixture was stirred until obtaining a homogeneous yellow solution which was heated in a water bath up to 343 K (solution C).

Titanium hydrolysis was induced through water produced in the esterification reaction between ethanol and a carboxylic acid with 1:1 molar ratio. Acetic acid (Scharlau, HPLC-grade) and formic acid (Scharlau, 98%) were selected for that purpose. In more detail, 1.050 mol of carboxylic acid and 0.054 mol of sulfuric acid (Sigma-Aldrich, 95–97%) were added dropwise to solution C. The resulting solution was stirred for 180 min, keeping constant the bath temperature at 343 K. The final white gel was filtered and dried overnight at 353 K in air atmosphere. Samples were calcined at different temperatures between 823 and 1023 K for 6 h (calcination rate of 1.8 K min^{-1}, starting at room temperature). Table 1 summarizes the synthesis specifications of the TiO_2 materials.

2.2. Photocatalytic experiments

The photocatalytic performance of TiO_2 materials obtained was assessed through the degradation of 10 mg L^{-1} MIT in Milli-Q® water, at natural pH (4.5). Commercial TiO_2 P25 (Evonik) was used as catalyst reference. The reactions were carried out in a borosilicate glass cylindrical reactor (1.4 L, 18.5 cm of internal diameter) filled with 1 L of MIT and catalyst suspension. The catalyst dosage was set as 0.5 g L^{-1}. The reactor was placed inside a solar simulator (Solarbox 1500 standard, CO. FO.ME.GRA, Italy) provided with a 1500 W Xenon Lamp and a cutoff filter for $\lambda < 300$ nm. The total irradiance between 300 and 800 nm was estimated to be 328.7 W m^{-2}. The suspension was magnetically stirred and bubbled with air during the reaction. For the quantitative analysis, samples were collected at different reaction times and filtered with a 0.45 μm Nylon filter for their injection in the liquid-chromatography instrument.

The effect of sulfate radicals on the photocatalytic reactions was investigated by adding sodium persulfate (EssentQ®, Scharlau) into the MIT reaction solution. The persulfate concentration was fixed at 2 mM based on previous reports [12,15].

To investigate the reusability of the catalyst, it was recovered after the reaction using a vacuum filtration system with a 0.2 μm filtering membrane. The catalyst was washed several times with ultrapure water and dried for 24 h in an oven at 363 K before reuse. The recovered material was then tested for two more cycles.

To evaluate the effect of the water matrix in the MIT photocatalytic degradation similar reactions were carried out using water obtained from the local drinking water supply (tap-water, TW) and water from a secondary effluent (SW), collected at a sewage treatment plant located in Móstoles (Madrid, Spain).

2.3. Analytical procedures

2.3.1. Catalysts characterization

The formation of crystalline phases of photocatalytic materials was determined by powder X-Ray Diffraction (XRD) (Philips X'PERT MPD) with Cu Kα radiation (λ = 1.5418 Å) at scan range of 2θ= 5–90 °, a step size of 0.01° and 1 s per step. Specific Surface Area (Brunauer-Emmett-Teller, S_{BET}) was estimated from the N_2 adsorption-desorption isotherms at 77 K, which were obtained using a Micromeritics® Tristar3000 instrument. FEG-SEM (Nova Nano SEM230) was employed for evaluating the particles morphology.

2.3.2. HPLC-DAD

The removal of MIT as a function of the irradiation time was followed using an HPLC-DAD system (Agilent 1260 Infinity II), equipped with a Poroshell 120 EC-C18 column (4.6 ×100 mm, Ø=2.7 μm) and a Diode-Array Detection DAD. The mobile phase consisted in a 90:10 mixture of methanol and acetic acid (0.1%) in isocratic mode at a flow rate of 0.8 mL min^{-1}. The injection volume was 20 μL and the DAD operated at 274 nm.

2.3.3. HPLC-HRMS

Samples collected from the photocatalytic experiments with TiO_2-A3 material and MIT were analyzed by HPLC-HRMS to identify MIT TPs. The Ultimate 3000 HPLC system (Thermo Scientific, Italy) was equipped

Table 1
Synthesis conditions of TiO_2 catalysts, BET area of samples and their pseudo-first order kinetic rate constants (k) and regression coefficient (R^2) values for MIT degradation reactions.

Procedure		Sample	$T_{calcination}$ (K)	BET ($m^2\ g^{-1}$)	k (min^{-1})	R^2
via esterification reaction	Acetic acid and ethanol	TiO_2-A1	823	31.8	0.0699	0.963
		TiO_2-A2	873	37.4	0.1086	0.962
		TiO_2-A3	923	45.2	0.1156	0.955
		TiO_2-A4	1023	10.5	0.0355	0.972
	Formic acid and ethanol	TiO_2-F1	823	17.3	0.0077	0.989
		TiO_2-F2	923	9.1	0.0081	0.993
Direct addition of water		TiO_2-W1[a]	823	35.2	0.0228	0.991
		TiO_2-W2[a]	923	38.9	0.0295	0.984
		TiO_2-W3	923	3.7	0.0087	0.971

[a] TiO_2-W1 and TiO_2-W2 were synthesized at a hydrolysis temperature of 273 K.

with a Restek Pinnacle DB Biphenyl column 150 × 2.1 mm with a particle size of 3 μm. Injection volume was 20 mL and flow rate 0.2 mL min^{-1}. The mobile phase consisted in an initial 95:5 mixture of methanol and formic acid (0.1 %) in a linear gradient mode. LTQ Orbitrap mass spectrometer (Thermo Scientific, Germany) equipped with an ESI ion source was used as a detector. Samples were analyzed in negative ion mode. Nitrogen was employed as sheath and auxiliary gas for delivering the LC column effluent into the ion source. The capillary voltage of the ESI source was 37.00 V, and its temperature was kept at 543 K. The source voltage was established at 3.5 kV and the collision energy was fixed at 30 (arbitrary units).

2.3.4. Total organic carbon analyzer

Shimadzu TOC-5000 analyzer (catalytic oxidation on Pt/Al_2O_3 quartz reactor at 953 K) was employed for measuring TOC in samples of MIT solution at different irradiation times in photocatalytic experiments.

2.3.5. Acute toxicity measurements

Samples toxicity was evaluated through the measurement of bioluminescence inhibition of *Vibrio Fischeri* using a Microtox® Model 500 Toxicity Analyzer (Milan, Italy). Changes in the natural emission of the bacteria can be monitored in the presence of toxic compounds. For the measurements, freeze-dried bacteria, reconstitution solution (2% NaCl) and an adjustment solution (non-toxic 22% sodium chloride) were employed (Azur, Milan, Italy). Luminescence of samples was recorded after 5, 15 and 30 min of incubation at 288 K.

3. Results and discussion

3.1. Catalyst characterization

Fig. 1 shows the X-ray diffraction (XRD) patterns of representative TiO_2 samples. All materials showed the characteristic diffraction peaks of anatase phase, with the main peak located at °2θ= 25.35, indexed to (101) (JCPDS Card No. 21–1272). Only TiO_2-A4 and TiO_2-W3 showed the peaks ascribed to rutile phase as main diffractions (2θ=27.45°, indexed to (110), JCPDS Card No. 21-1276). Comparing both procedures for n-butoxide hydrolysis, the hydrolysis temperature (273 and 343 K) determined the main formation of anatase or rutile at a calcination temperature of 923 K in the case of the external addition of water (TiO_2-W2 and TiO_2-W3, respectively) whereas calcination temperatures above 923 K were necessary to promote the formation of rutile when water for hydrolysis was provided *in situ* (TiO_2-A4).

BET area values are displayed in Table 1. Evident differences between TiO_2-A3 and TiO_2-F2 can be observed. SEM images are collected in Fig. S1 in Supplementary Information. All selected samples showed spherical morphologies. Using acetic acid in the esterification reaction

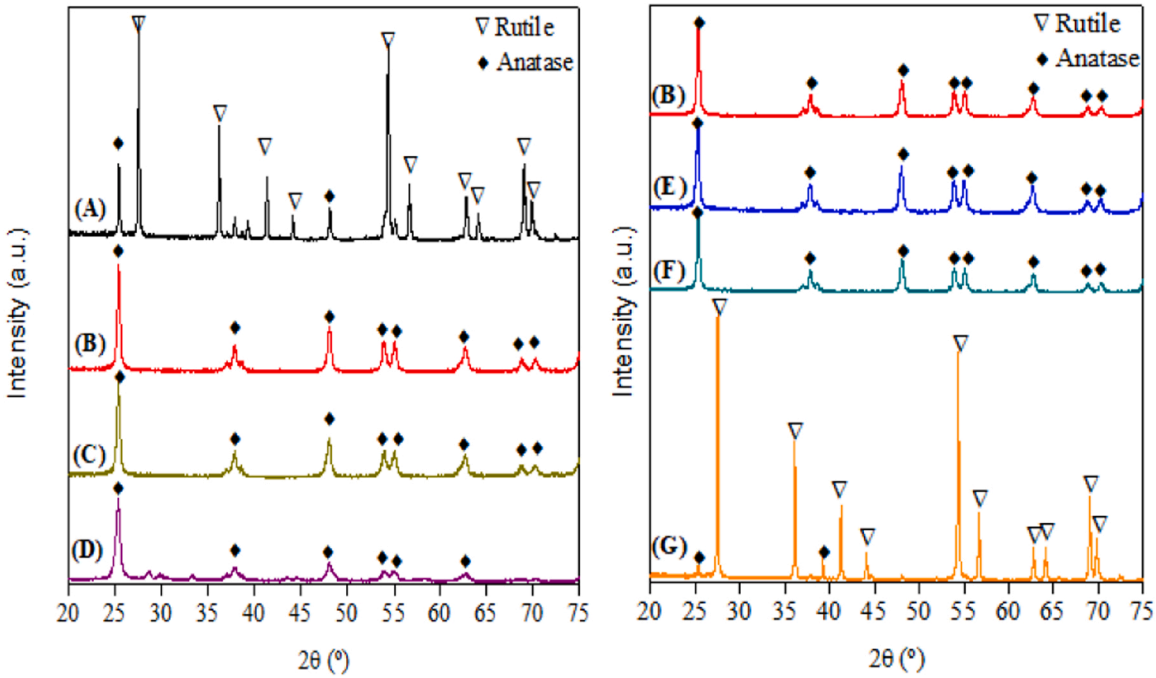

Fig. 1. XRD patterns of (A) TiO_2-A4, (B) TiO_2-A3, (C) TiO_2-A2, (D) TiO_2-A1, (E) TiO_2-F2, (F) TiO_2-W2 and (G) TiO_2-W3.

during the sol-gel synthesis resulted in the formation of small particles of anatase-TiO_2 with the highest BET area. Furthermore, the comparison between TiO_2-W2 and TiO_2-W3 proved that the synthesis at 343 K induced in the latter the formation of big nano-particles agglomerations.

3.2. Photocatalytic activity

TiO_2 materials were tested for MIT degradation in Milli-Q® water and compared with the commercial P25 catalyst. Prior to the photocatalytic reactions, preliminary experiments were done to evaluate the extent of the organic compound adsorption on TiO_2 by keeping the MIT solution in contact with the catalyst for 120 min in dark conditions. No appreciable MIT adsorption was observed for any of the samples. As it is shown in Fig. 2. (A), among TiO_2-A samples, TiO_2-A3 showed the highest photocatalytic activity achieving the complete removal of the pollutant in 30 min, even outperforming P25. The MIT concentration profile attained with TiO_2-A4 indicated that the increase of the calcination temperature with the subsequent decrease of BET area and rutile formation, was detrimental for its efficiency as a catalyst. Even so, most of the selected materials exhibited a great ability for the total abatement of MIT in water, reaching the complete removal of the compound in less than 60 min of reaction.

The kinetics of the photocatalytic degradation followed a pseudo-first order reaction. Thus, Fig. 2 (B) depicts a comparison of the calculated kinetic constant values for MIT degradation employing some of the synthesized catalysts and the reference material (P25). The highest activity was observed with the material synthesized by using acetic acid in the esterification reaction.

The production of water due to the esterification reaction between the carboxylic acid and ethanol (Eq. (2)) could be a way of controlling the hydrolysis of titanium butoxide (Eq. (3)). In these terms, the esterification kinetic constant (K_E) plays a key role in the rate of water provision for the hydrolysis reaction. Accordingly, the significant difference in the K_E values for the reactions between the chosen organic acids and ethanol at 343 K (21.787×10^5 dm^3 mol^{-1} s^{-1} for formic acid and 2.671×10^5 dm^3 mol^{-1} s^{-1} for acetic acid [16]) could explain the distinctive photocatalytic results obtained with TiO_2-F2 and TiO_2-A3 related to their different BET areas (9.1 m^2 g^{-1} *vs* 45.2 m^2 g^{-1}, respectively), which revealed the importance of the esterification rate in the final specific surface area of the resulting materials. A rapid production of H_2O from the esterification likewise results in a fast hydrolysis of titanium alkoxide.

$$RCOOH + CH_3CH_2OH \xrightarrow{H_2SO_4} RCOOR' + H_2O \quad (2)$$

$$Ti(OBu)_4 + 4H_2O \rightarrow Ti(OH)_4 + 4(BuOH) \quad (3)$$

On the other hand, the direct addition of water into the titanium butoxide solution led to an even faster hydrolysis rate, which could be controlled by the temperature of the system since the lower the synthesis temperature, the slower the kinetics of the alkoxide hydrolysis reaction. Thus, the comparison of TiO_2-W2 and TiO_2-W3 photoactivity confirmed the influence of the synthesis temperature on the textural, crystalline and photocatalytic properties of the materials obtained. A slower hydrolysis rate of the titanium alkoxide led to an enhancement in the catalyst performance due to a higher surface area and the formation of anatase as main crystalline phase.

3.3. Identification of transformation products (TPs)

TPs identified throughout the photocatalytic reaction of MIT with TiO_2-A3 are collected in Table. S1. Accordingly, a possible degradation pathway of the molecule was proposed. As Fig. 3 shows, in the first stage of the reaction, the $HO^{\bullet}$ attack to the organic molecule leads to the formation of the intermediate $C_4H_5NO_2S$ which evolves *via* tautomerization to the cyclic diketone. The opening of the heterocycle, which involves the loss of sulfur atom, leads to the formation of N-methylmalonamic acid ($C_4H_7O_3N$). After that, other linear chain products with amine and dicarboxylic groups, as malonamic acid ($C_3H_5O_3N$) and malonic acid ($C_3H_4O_4$) are formed, leading to the consequent transformation to acetic acid and formic acid, which finally decompose into H_2O, CO_2 and HCO_3^-.

3.4. Acute toxicity and mineralization

The initial MIT water solution induced 100 % of bacteria luminescence inhibition (Fig. 4), hence evidencing the high toxicity of MIT even at low concentration. During the reaction, both luminescence inhibition and TOC curve decreased although the profile of toxicity indicates the formation of intermediates more toxic than their precursors after 45 min. Nevertheless, the final low percentage of effect on bacteria (~2 %), indicates the non-toxicity of the water solution after the treatment, also supported by the TOC analysis, reaching the total mineralization of MIT after 2 h of irradiation.

3.5. Activation of persulfate

The effect of PS addition to the TiO_2 photocatalytic system was also evaluated. Adding 2 mM PS to the suspension of MIT and the titania catalyst greatly increased the degradation rate of the pollutant as it can be observed in Fig. 5. For TiO_2-A3, MIT removal was completed in 15 min of irradiation exposure, in comparison to 75 % of degradation achieved without PS addition. The same concentration of PS was also tested in the absence of catalyst, achieving the removal of 33 % of the

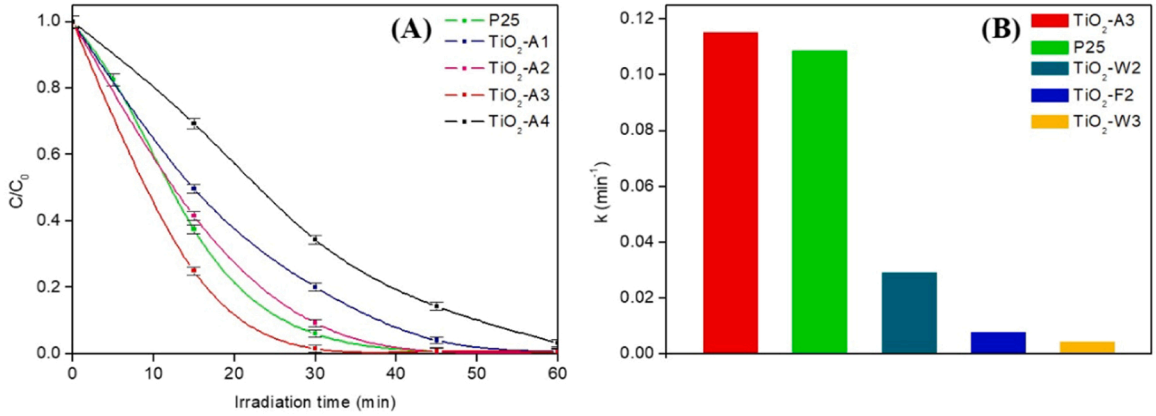

Fig. 2. (A) Influence of calcination temperature on the photocatalytic activity of TiO_2-A materials for MIT degradation in Milli-Q® water, and (B) comparison of the kinetic constants of the photocatalytic reaction with selected samples.

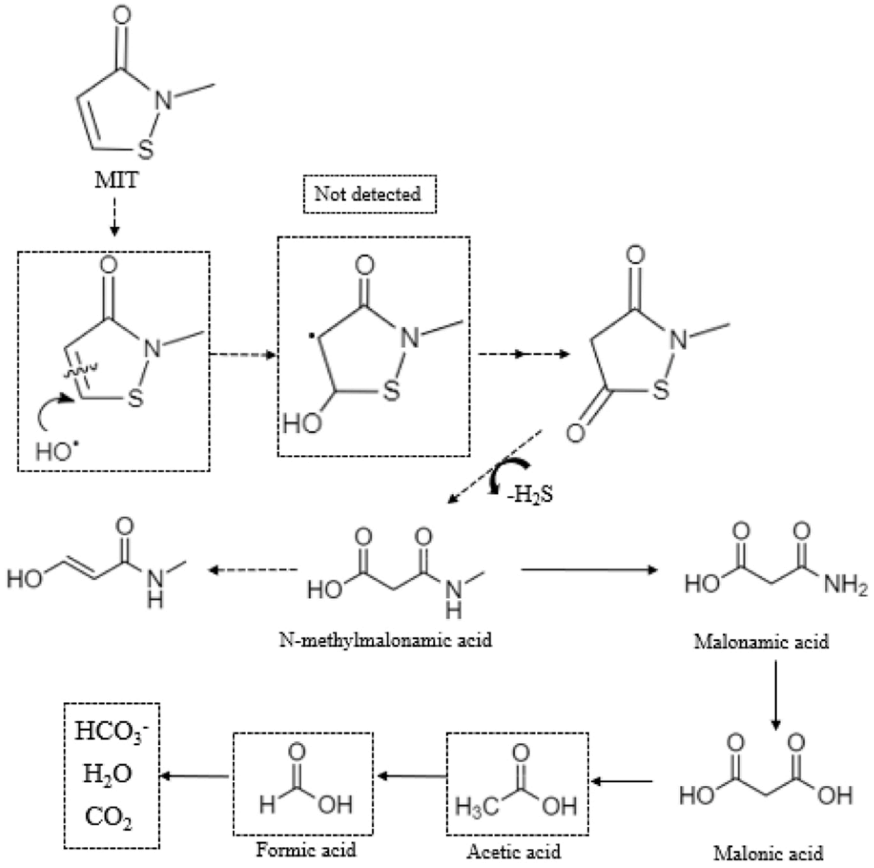

Fig. 3. Degradation pathway of MIT with TiO_2-A3 catalyst in Milli-Q® water.

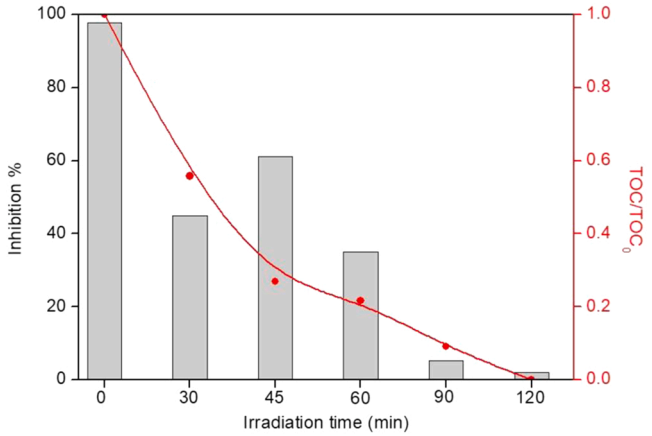

Fig. 4. Acute toxicity and TOC profiles over time for the reaction of MIT degradation with TiO_2- A3.

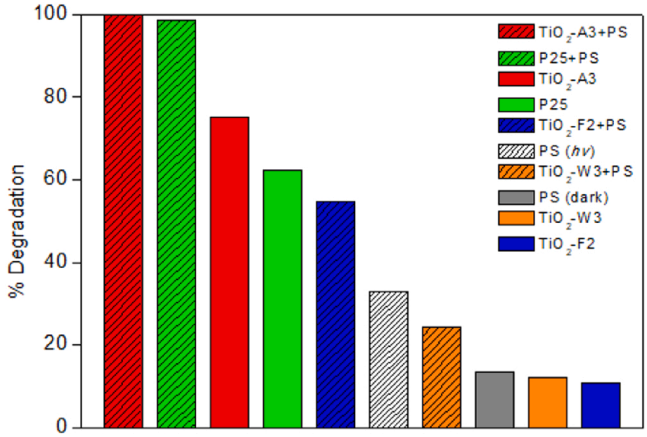

Fig. 5. Effect of 2 mM PS addition on catalysts performance for MIT degradation after 15 min of irradiation.

initial concentration of MIT.

To evaluate if the enhancement of activity was related to a synergistic effect between the catalyst and PS, a synergy factor was calculated for each experiment following Eq. (4):

$$\text{Synergy}_{A+B} = \frac{k_{A+B}}{k_A + k_B} \quad (4)$$

A synergistic effect is achieved when the calculated factor value is greater than 1, whereas an antagonistic effect occurs with values lower than 1, which would mean a negative effect of the sum of processes [17]. Table 2 summarizes the kinetic constants and the synergy factor values obtained. TiO_2-W3 sample was the only one showing an antagonistic

Table 2
Values of the kinetic rate constants (k) and synergy factors for MIT photocatalytic degradation.

Sample	Water Matrix	k (min^{-1})	k (min^{-1}) (PS addition)	Synergy
TiO_2-A3	Milli-Q®	0.1156	0.2027	1.3770
	TW	0.0276	0.1171	2.1175
	SW	0.0127	0.0321	1.9222
P25	Milli-Q®	0.1089	0.1916	1.3637
	TW	0.0252	0.1059	1.9721
	SW	0.0123	0.0236	1.4479
TiO_2-F2	Milli-Q®	0.0081	0.0531	1.3375
TiO_2-W3	Milli-Q®	0.0046	0.0175	0.4834

effect when adding PS. The low photocatalytic activity showed for MIT abatement with this sample upon PS addition, seemed to be related with the rutile crystallinity of the sample, which would not be able to effectively promote the activation of persulfate under solar radiation. In addition, the decrease of the reaction rate observed in the system (TiO_2-W3 + PS) compared to (PS-hν) may be attributed to the light shielding effect of TiO_2-W3 particles which diminishes the direct UV-activation of PS.

3.6. Application in real water matrix

To evaluate the influence of the water matrix on the performance of TiO_2-A3 for MIT degradation, reactions without and with PS were carried out using tap-water, TW, (COD=2.5 mg L^{-1}, TOC=9.4 mg L^{-1}) and water collected from the secondary effluent at a sewage treatment plant, SW (COD=17.6 mg L^{-1}, TOC= 46.2 mg L^{-1}). Table 2 displays the pseudo-first order kinetic constants calculated for MIT degradation in these experiments and the comparison with the reference TiO_2 P25 (degradation curves are shown in Fig. S2). The decrease of the reaction rate in TW and SW matrices can be attributed to the presence of naturally occurring scavengers such as dissolved organic matter, Cl^-, HCO_3^-, and SO_4^{2-}, which can act as radical scavengers of the photogenerated radicals [18]. The reduction of TOC with the irradiation time was also slowed down in TW and SW matrices compared to Milli-Q® water. A decrease of TOC below the detection limit was attained after 4.5 h in the TW matrix, whereas a diminution of 81 % initial TOC was measured after 8 h in the SW matrix. Nevertheless, the results corroborate the good performance of the TiO_2-A3 sample in real water matrices which can be boosted by the introduction of persulfate into the photocatalytic system. As shown in Table 2, adding 2 mM persulfate enhanced the MIT degradation rate in all cases being the synergistic effect more pronounced for TW and SW matrices compared to Milli-Q® water.

3.7. Catalyst reuse

The use of TiO_2-A3 catalyst in increasing number of catalytic cycles showed no loss of activity after the 2nd and a slight decrease in the reaction rate after the 3rd cycle ($k_{1st\ cycle}$= 0.1156 min^{-1}; $k_{2nd\ cycle}$ = 0.1127 min^{-1}; $k_{3rd\ cycle}$= 0.0850 min^{-1}) (Fig. S3). In each cycle, the separation process meant the loss of approximately 4% of initial content of catalyst, which could be also related to the small decrease of activity in the third reuse. However, TiO_2-A3 successfully achieved a complete degradation of the pollutant in less than 60 min of irradiation exposure after its recovery. These results confirmed the capability of TiO_2-A3 for being reused at least three times without losing its efficiency drastically, which would allow to reduce costs in the catalyst production for water treatment.

4. Conclusions

In the present study, the abatement of MIT in water under simulated solar radiation was investigated with different TiO_2 catalysts synthesized by the sol-gel method, using different strategies for attaining the hydrolysis of the titanium precursor. Controlling the hydrolysis rate of titanium alkoxide through an esterification reaction with acetic acid and ethanol resulted in a catalyst with the highest BET area and the greatest photocatalytic activity for MIT abatement, even in real water matrices. The addition of PS enhanced the reaction rate in all cases proving the high efficiency of sulfate radicals in the degradation of the organic compound. Recovery and reuse of the catalyst were successfully tested. MIT TPs were identified, and TOC and acute toxicity measurements revealed the non-toxicity of water solution after the photocatalytic reaction therefore, proving the successful performance of TiO_2 and TiO_2/PS for attaining the treatment of water polluted with MIT.

CRediT authorship contribution statement

Pilar Gómez-Rodríguez: Investigation, Conceptualization, Writing – original draft. **Paola Calza:** Funding acquisition, Writing – review & editing. **Debora Fabbri:** Investigation, Writing – review & editing. **Claudio Medana:** Writing – review & editing. **Rafael van-Grieken:** Supervision, Writing – review & editing. **María José López-Muñoz:** Conceptualization, Supervision, Writing – review & editing, Funding acquisition.

Declaration of Competing Interest

The authors declare that they have no known competing financial interests or personal relationships that could have appeared to influence the work reported in this paper.

Data Availability

Data will be made available on request.

Acknowledgements

The authors would like to acknowledge the financial support of the "Agencia Estatal de Investigación" (AEI) and the "Ministerio de Ciencia, Innovación y Universidades" through the project CALYPSOL (RTI2018-097997-B-C33) and funding from the European Union's Horizon 2020 Research and Innovation Programme under the Marie Skłodowska-Curie grant agreement No 101007578 (SusWater).

Appendix A. Supporting information

Supplementary data associated with this article can be found in the online version at doi:10.1016/j.cattod.2022.11.003.

References

[1] V. Silva, C. Silva, P. Soares, E.M. Garrido, F. Borges, J. Garrido, Isothiazolinone biocides: chemistry, biological, and toxicity profiles, Molecules 25 (2020), https://doi.org/10.3390/molecules25040991.
[2] A. Herman, O. Aerts, L. de Montjoye, I. Tromme, A. Goossens, M. Baeck, Isothiazolinone derivatives and allergic contact dermatitis: a review and update, J. Eur. Acad. Dermatol. Venereol. 33 (2019) 267–276, https://doi.org/10.1111/jdv.15267.
[3] P. Speksnijder, J. van Ravestijn, P. de Voogt, Trace analysis of isothiazolinones in water samples by large-volume direct injection liquid chromatography tandem mass spectrometry, J. Chromatogr. A 1217 (2010) 5184–5189, https://doi.org/10.1016/j.chroma.2010.06.010.
[4] Regulation (EC) No 1223/2009 of the European Parliament and of the Council of 30 November 2009 on cosmetic products, (n.d.) 151.
[5] J. Marugán, M.J. López-Muñoz, P. Fernández-Ibáñez, S. Malato, Solar photocatalysis: fundamentals, reactors and applications. RSC Energy and Environment Series, The Royal Society of Chemistry, Cambridge, 2016, pp. 92–129.
[6] D. Chen, Y. Cheng, N. Zhou, P. Chen, Y. Wang, K. Li, S. Huo, P. Cheng, P. Peng, R. Zhang, L. Wang, H. Liu, Y. Liu, R. Ruan, Photocatalytic degradation of organic pollutants using TiO_2-based photocatalysts: a review, J. Clean. Prod. 268 (2020), 121725, https://doi.org/10.1016/j.jclepro.2020.121725.
[7] M.J. López-Muñoz, A. Revilla, G. Alcalde, Brookite TiO_2-based materials: Synthesis and photocatalytic performance in oxidation of methyl orange and As(III) in aqueous suspensions, Catal. Today 240 (2015) 138–145, https://doi.org/10.1016/j.cattod.2014.05.008.
[8] G. Marcì, L. Palmisano. Heterogeneous Photocatalysis: Relationships with Heterogeneous Catalysis and Perspectives, first ed., Elsevier, Amsterdam, 2019 https://doi.org/10.1016/C2016-0-04769-1.
[9] W.-D. Oh, Z. Dong, T.-T. Lim, Generation of sulfate radical through heterogeneous catalysis for organic contaminants removal: current development, challenges and prospects, Appl. Catal. B: Environ. 194 (2016) 169–201, https://doi.org/10.1016/j.apcatb.2016.04.003.
[10] J. Wang, S. Wang, Activation of persulfate (PS) and peroxymonosulfate (PMS) and application for the degradation of emerging contaminants, Chem. Eng. J. 334 (2018) 1502–1517, https://doi.org/10.1016/j.cej.2017.11.059.
[11] J. Scaria, P.V. Nidheesh, Comparison of hydroxyl-radical-based advanced oxidation processes with sulfate radical-based advanced oxidation processes, Curr. Opin. Chem. Eng. 36 (2022), 100830, https://doi.org/10.1016/j.coche.2022.100830.

[12] M. Ge, Z. Hu, J. Wei, Q. He, Z. He, Recent advances in persulfate-assisted TiO_2-based photocatalysis for wastewater treatment: performances, mechanism and perspectives, J. Alloy. Compd. 888 (2021), 161625, https://doi.org/10.1016/j.jallcom.2021.161625.

[13] D.M. EL-Mekkawi, A.A. Labib, H.A. Mousa, H.R. Galal, W.A.A. Mohamed, Preparation and characterization of nano titanium dioxide photocatalysts via sol gel method over narrow ranges of varying parameters, Orient. J. Chem. 33 (2017) 41–51, https://doi.org/10.13005/ojc/330105.

[14] J. Zhu, J. Zhang, F. Chen, K. Iino, M. Anpo, High activity TiO_2 photocatalysts prepared by a modified sol–gel method: characterization and their photocatalytic activity for the degradation of XRG and X-GL, Top. Catal. 35 (2005) 261–268, https://doi.org/10.1007/s11244-005-3833-1.

[15] A. Gabet, H. Métivier, C. de Brauer, G. Mailhot, M. Brigante, Hydrogen peroxide and persulfate activation using UVA-UVB radiation: degradation of estrogenic compounds and application in sewage treatment plant waters, J. Hazard. Mater. 405 (2021), 124693, https://doi.org/10.1016/j.jhazmat.2020.124693.

[16] Y.A. Elewady, M. El-Nahas, M.N.H. Moussa, Kinetics of Esterification of Some Organic Acids with Ethanol Using Amberlite IR-120 as Catalyst, (n.d.) 3.

[17] S. Mesones, E. Mena, M.J. López-Muñoz, C. Adán, J. Marugán, Synergistic and antagonistic effects in the photoelectrocatalytic disinfection of water with TiO_2 supported on activated carbon as a bipolar electrode in a novel 3D photoelectrochemical reactor, Sep. Purif. Technol. 247 (2020), 117002, https://doi.org/10.1016/j.seppur.2020.117002.

[18] J. Plaza, A. Arencibia, M.J. López-Muñoz, Evaluation of nZVI for the degradation of atrazine in heterogeneous Fenton-like systems at circumneutral pH, J. Environ. Chem. Eng. 9 (2021), 106641, https://doi.org/10.1016/j.jece.2021.106641.